Journal of Ovonic Research Vol. 16, No.. 3, May - June 2020, p. 165 - 171

IMPACT OF Ni DOPANT ON OPTICAL AND MAGNETIC PROPERTIES OF ZnO NANOPARTICLES FOR BIOMEDICAL APPLICATIONS

T. MUNIR*, A. MAHMOOD, M. KASHIF, A. SOHAIL, M. S. SHIFA, M. SHARIF, S. MANZOOR
Department of Physics, Government College University Faisalabad (GCUF), Allama Iqbal Road, Faisalabad, 38000, Pakistan

In this work, $Zn_{1-x}Ni_xO$ NPs with different concentration (x= 0.0, 0.03, 0.06 and 0.09) were synthesized by using co-precipitation method. The present study is related to investigate crystal structure, surface morphology, optical and magnetic behavior of pure and Ni dopant ZnO NPs. The hexagonal wurtzite structure and crystallite size (19.45 to 21.25 nm) was investigated by using XRD analysis.SEM and FTIR used to identify the surface morphology, stretching and vibrational modes of different functional groups (ZnO, OH, CO and H-O-H) attached on the spectrum of Ni dopant ZnO NPs. Moreover, the optical behavior of Ni dopant ZnO NPs was studied by UV-visible spectroscopy which indicates the absorption band of red shift. Finally, VSM analysis illustrated that Ni dopant ZnO NPs shows high magnetization, retentivity and low corecivity as compare to pure ZnO NPs. In an overall assessment the Ni dopant ZnO NPs shows better optical and magnetic properties for biomedical applications.

(Received February 3, 2020; Accepted June 1, 2020)

Keywords: Ni Dopant ZnO NPs, Hexagonal wurtzite, Optical absorption, Magnetization, Biomedical applications.

1. Introduction

With the advancements in medical sciences, the way of treatment for different diseases has been revolutionized dramatically over the last few decades. Diseases, which were considered horrible in the past, are now treatable. The antibiotic medication causes some side effect for living organs. The nanomaterials science is helping out to solve these critical issues very carefully without damaging the internal organs [1, 2]. Furthermore, the metal NPs due to unique physical, chemical and biological properties are preferred for biomedical applications (cancer, antibacterial and skin treatment) [3-5].

The interest in ZnO NPs is fueled and stimulated by its excellent characteristics such as biocompatibility, excellent thermodynamic stability, preferable wide bang gap (3.36 eV) and high binding energy (60 meV) which makes ZnO NPs excellent candidate for diverse applications. Recently, the researchers used transition dopant metal (Mn, Co, Fe, Ni etc) to enhance the properties of ZnO NPs. Moreover, dopant ZnO NPs were played the central role in PDT, PTT and hyperthermia therapy for the treatment of cancer [6-8].The preferred choice of nickel dopant in ZnO NPs instead of other transition metals is due to ionic radius of nickel ion (0.69Å) is much close to zinc ion (0.74 Å) and same valency of Ni^{+2} and Zn^{+2} ion. Therefore, Ni ion favorable to substitute Zn ion [9,10]. Furthermore, the production of fee radical such as Ni^{+2} and Zn^{+2} used to kill the bacteria most helpful for antibacterial activity [11, 12].

Currently, variety of methods were used to synthesize the metal oxide NPs for biomedical applications such as green synthesis, sol gel, co-precipitation method and many more. In this research work the main focus is co-precipitation method due to ecofriendly environment, small and uniform particles size preparation. The goal of this research work was to study the impact of Ni dopant on optical and magnetic properties of ZnO NPs using different characterization techniques (XRD, SEM, FTIR, UV-visible spectroscopy and VSM). It is expected that Ni dopant ZnO NPs are most beneficial for biomedical applications.

* Corresponding author: tariqmunir@gcuf.edu.pk

2. Experimental procedures

2.1. Synthesis method for ZnO NPs

Co-precipitation method was used to synthesize ZnO NPs. For this purpose, zinc nitrate hexahydrate (0.024M) solution was dissolved in de-ionize water of 350 mL and continue stirring for 3 hour at 60°C on magnetic stirrer. Furthermore, the sodium carbonate (0.1M) and sodium hydroxide (0.1M) was used to prepared the buffer solution in 50 mL de-ionize water. After that the buffer solution added in zinc nitrate hexahydrate solution to attain the pH of solution. Then the final product white color solutions obtained and solution was filtered by using the filter paper and then dried in oven for 200°C. After that the ZnO product was annealed at 500 ^{0}C for 5 hour inside furnace.

2.2. Synthesis method for Ni doped ZnO NPs

The direct addition was used to synthesize Ni doped ZnO NPs. Nickel (II) nitrate hexahydrate (0.001, 0.002, 0.003 M) concentration was mixed in 10 mL de-ionized water continue stirring for 30 min on magnetic stirrer. After that Ni solution added into ZnO solution then the final product Ni doped zinc oxide NPs was obtained. The final product was dried and grinded using the mortar and pestle.

3. Results and discussion

3.1 XRD analysis

Fig.1 indicates the XRD spectrum of pure and Ni doped ZnO NPs. The graph shows that there is no secondary peak of Ni or NiO at low concentration of x below 0.03. Moreover, at Ni concentration (x=0.03) indicate the presence of NiO peak at angle 43^0 as it increases from (0.03 to 0.09) which indicate that Ni ion substitute Zn ion. Hexagonal wurtzite structure of pure and Ni doped ZnO NPs appeared [13-15]. Furthermore, Table 1 shows d spacing and crystallite size calculated by using following equations.

$$d_{hkl} = \frac{\lambda}{2\sin\theta} \text{.....} (I) \quad D = \frac{k\lambda}{\beta\cos\theta} \text{.....} (II)$$

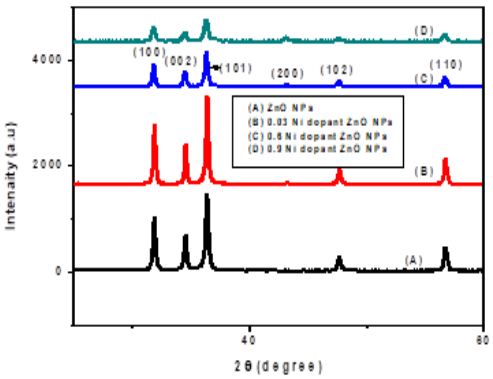

Fig. 1.XRD spectrum of pure and Ni-doped ZnO NPs.

Table 1.Variation of crystallite size and d-spacing of Ni dopant ZnO NPs.

Miller indices hkl	d (inter plane distance)	Crystallite size (nm)
100	2.8	19.45
002	2.6	19.58
101	2.476	19.68
200	2.10	20.11
102	1.9	20.45
110	1.6246	21.25

3.2. SEM analysis

Fig. 2 shows the surface morphology of pure and Ni doped ZnO NPs. SEM analysis indicate that ZnO NPs were irregular, non-uniform, small and large sphere. As the nickel concentration increases in ZnO, particles were obtained with regular shape and uniform size. Therefore, the concentration of nickel reduced the agglomeration of Ni doped ZnO NPs [16-17].

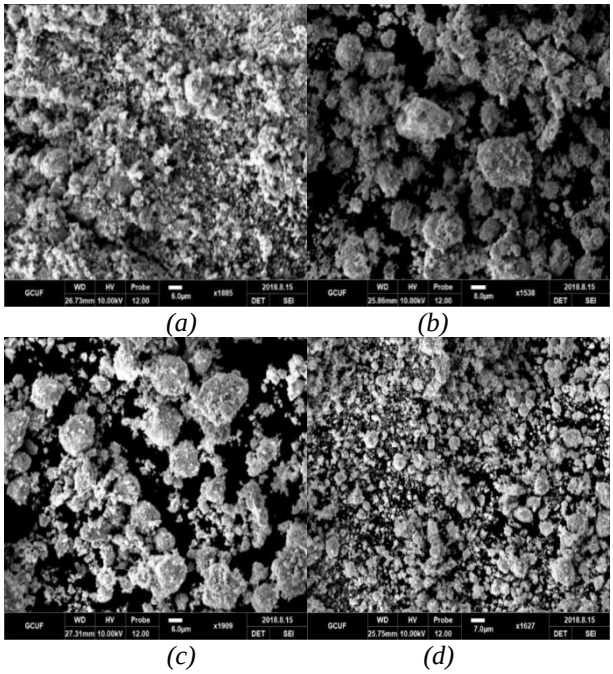

Fig. 2. SEM micrograph of:(a) Pure ZnO NPs; (b) 0.03 Ni dopant ZnO NPs; (c) 0.06 Ni dopant ZnO NPs; (d) 0.09 Ni dopant ZnO NPs

3.3. FTIR analysis

Fig. 3 indicates the transmittance of pure and Ni dopant ZnO NPs. It was found that Ni concentration does not change the spectra. The different stretching and vibrational mode of functional groups attached on ZnO NPs were observed and listed in Table 2.These functional groups were most suitable for all living organs [18-20].

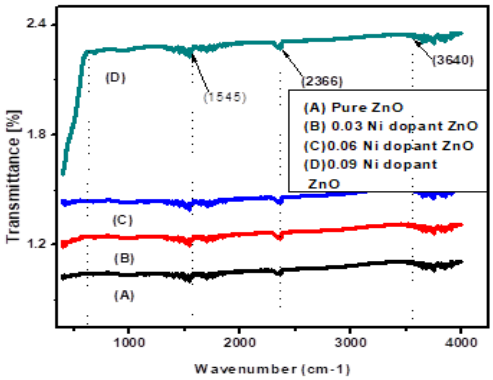

Fig. 3.FTIR spectrum of pure and Ni dopant ZnO NPs.

Table 2.FTIR spectra of pure and Ni dopant ZnO NPs.

Bands	ZnO	$ZnNi_{0.03}O$	$ZnNi_{0.06}O$	$ZnNi_{0.09}O$
Zn-O Stretching	411-674 cm-1	405-672 cm-1	415-671 cm-1	405-672 cm-1
H-O-H Vibration stretching	1543-1694 cm-1	1545-1698 cm-1	1545-1698 cm-1	1545 cm-1
CO stretching	2362 cm-1	2356 cm-1	2358 cm-1	2366 cm-1
O-H Stretching	3650 cm-1	3660 cm-1	3650 cm-1	3651 cm-1

3.3. UV-visible spectroscopy analysis

Fig. 4 indicates optical absorption peaks in the range of 200 nm to 600 nm of pure and Ni doped ZnO NPs. The absorption peaks of these NPs were observed in range 375-391nm.With addition of Ni dopant agent these peaks shifted towards longer wavelength (red shift) [21].

Table 3 illustrated the cut-off wavelength and band gap of pure and Ni dopant ZnO NPs. UV analysis shows that band gap decreases from 3.31 to 3.17 eV as the concentration of Ni doping agent increases in ZnO. Therefore, reduction in conduction band was evident as Ni concentration increases in ZnO NPs. Fig. 5 shows the relation between band gap and Ni concentration. Moreover, these optical properties of Ni dopant ZnO NPs favorable for the treatment of cancer cells by using PTT and PDT [22].

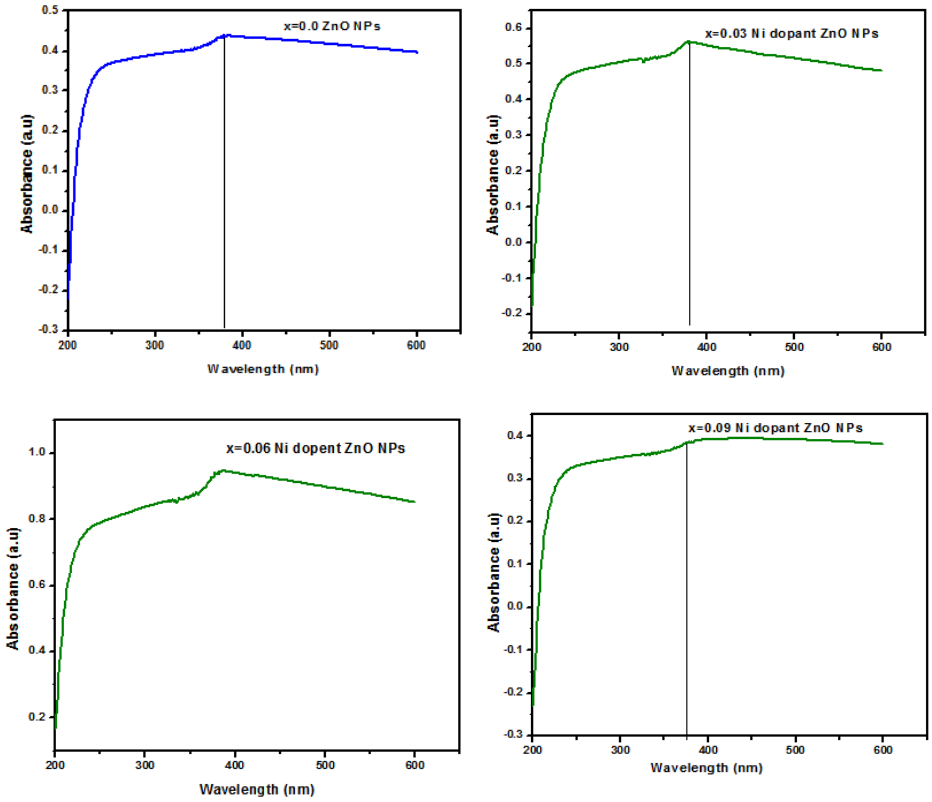

Fig. 4. Absorption band of pure and Ni dopant ZnO NPs.

Table 3. Cut-off wavelength and band gap values of pure and Ni dopant ZnO NPs.

X	Wavelength (nm)	Band Gap (eV)
0.00	375	3.31
0.03	378	3.28
0.06	381	3.26
0.09	391	3.17

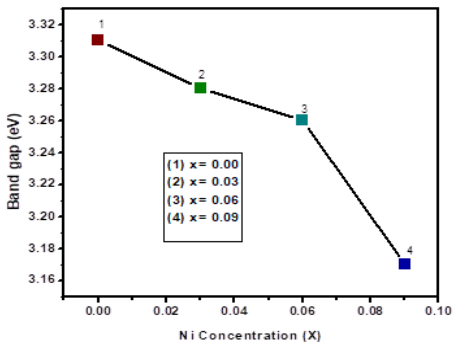

Fig. 5.Expression of band gap with concentration of Ni dopant ZnO NPs.

3.5. Vibrating Sample Magnetometry (VSM)

Fig. 6 shows hysteresis loop of pure and Ni dopant ZnO NPs. It indicates that as nickel contents increases in ZnO NPs, magnetization power increases. Ni dopant in ZnO NPs enhanced the ferromagnetic nature due to defects increases. Table 4: express the Ni doped ZnO NPs with

high magnetization, retentivity and low corecivity as compared to pure ZnO NPs [23, 24]. Recently, zinc ferrite was preferred for treatment of cancer by using hyperthermia therapy and drugs delivery [25]. The properties of Ni dopant ZnO NPs are most suitable for treatment of cancer cells.

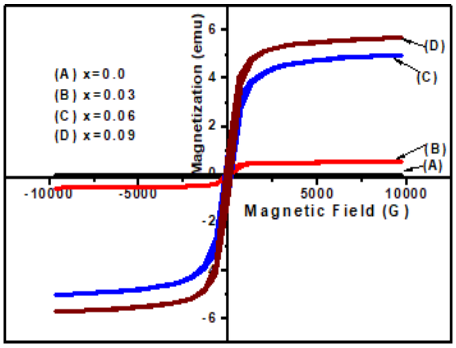

Fig. 6.VSM peaks of pure and Ni dopant ZnO NPs.

Table 4.VSM analysis of Ni dopant ZnO NPs.

Sample	**ZnO**	**$ZnNi_{0.03}O$**	**$ZnNi_{0.06}O$**	**$ZnNi_{0.09}O$**
Magnetization (Ms)	15.5691×10^{-3}emu	0.54354 emu	1.5786 emu	2.5634 emu
Retentivity (Mr)	1.0226×10^{-3}emu	1.6435×10^{-3}emu	0.81341 emu	0.69559 emu
Corecivity (Hci)	314.28 G	92.847 G	153.61 G	100.22 G

4. Conclusion

Pure and Nickel dopant ZnO NPs were successfully synthesized by using co-precipitation method. XRD analysis shows the hexagonal wurtzite crystalline structure and crystallite size varies from (19.45 to 21.25 nm). SEM analysis revealed improved surface morphology uniform, spherical and cluster shape while FTIR analysis verified that ZnO NPs IR spectra are not affected by nickel dopant. UV-Visible analysis indicated the red shift as Ni concentration increases in ZnO NPs. Finally, VSM analysis shows that nickel dopant ZnO NPs, high magnetization, retentivity, low corecivity and strong ferromagnetic nature as compared to pure ZnO NPs. Ni dopant ZnO NPs shows excellent optical and magnetic properties which will be most suitable for biomedical applications.

Acknowledgements

The authors would like to extend their sincere appreciation to HEC under Project Numbers 8466/Punjab/NRPU/R&D/HEC/2017 Dr Tariq Munir Department of Physics Government College University Faisalabad Pakistan.

References

[1] T. Munir, A. Mahmood, M. Fakhar-e-Alam, M. Imran, A. Sohail, N. Amin, S. Latif , H. G. Rasool, F. Shafiq, H. Ali, K. Mahmood, Journal of Molecular Structure, **1196**, 88-95(2019).
[2] R. Vinhas, M. Cordeiro, F. F. Carlos, S. Mendo, A. R. Fernandes, S. Figueiredo, P. V.Baptista, Nanobiosensors in Disease Diagnosis **4**, 11 (2015).
[3] H. Sharma, P. K. Mishra, S. Talegaonkar, B. Vaidya, Drug discovery today **20**(9), 1143 (2015).
[4] G. Bisht, S. Rayamajhi, Nanobiomedicine **3**, 3 (2016).
[5] E. A. Kamoun, E. R. S. Kenawy, X. Chen, Journal of advanced research **8**(3), 217 (2017).
[6] B. Ghaemi, O. Mashinchian, T. Mousavi, R. Karimi, S. Kharrazi, A. Amani, ACS applied Materials & interfaces **8**(5), 3123 (2016).
[7] A. F. Ismail, M. M. Ali, L. F. Ismail, Journal of Photochemistry and Photobiology B: Biology **138**, 99 (2014).
[8] J. W. Rasmussen, E. Martinez, P. Louka, D. G. Wingett, Expert opinion on drug delivery **7**(9), 1063 (2010).
[9] S. Husain, F. Rahman, N. Ali, P. A. Alvi, J.Optoelectron. Eng. **1**(1), 28 (2013).
[10] B. Pal, D. Sarkar, P. K. Giri, Applied Surface Science **356**, 804 (2015).
[11] M. Premanathan, K. Karthikeyan, K. Jeyasubramanian, G. Manivannan, Nanomedicine: Nanotechnology, Biology and Medicine **7**(2), 184 (2011).
[12] G. Applerot, A. Lipovsky, R. Dror, N. Perkas, Y. Nitzan, R. Lubart, A. Gedanken, Advanced Functional Materials **19**(6), 842 (2009).
[13] G. J. Huang, J. B. Wang, X. L. Zhong, G. C. Zhou, H. L. Yan, Journal of materials science **42**(15), 6464 (2007).
[14] B. Pal, D. Sarkar, P. K. Giri, Applied Surface Science **356**, 804 (2015).
[15] C. J. Cong, J. H. Hong, Q. Y. Liu, L. Liao, K. L. Zhang, Solid State Communications **138**(10-11), 511 (2006).
[16] S. Kant, A. Kumar, Adv. Mat. Let. **3**(4), 350 (2012).
[17] R. Elilarassi, G. Chandrasekaran, American Journal of Materials Science **2**(1), 46 (2012).
[18] G. Vijayaprasath, R. Murugan, T. Mahalingam, G. Ravi, Journal of Materials Science: Materials in Electronics **26**(9), 7205 (2015).
[19] G. Srinet, R. Kumar, V. Sajal, Journal of Applied Physics **114**(3), 033912 (2013).
[20] S. Fabbiyola, V. Sailaja, L. J. Kennedy, M. Bououdina, J. J. Vijaya, Journal of Alloys and Compounds **694**, 522 (2017).
[21] J. Eppakayala, M. R. Mettu, V. R. Pendyala, J. R. Madireddy, Materials Today: Proceedings, 2019.
[22] Y. Wang, X. Liao, Z. Huang, G. Yin, J. Gu, Y. Yao, Colloids and Surfaces A: Physicochemical and Engineering Aspects **372**(1-3), 165 (2010).
[23] I. Abood, A. A. Gadalla, I. Abood, M. M. Elokr, Journal of Nanotechnology and Materials Science **4**(1), 19 (2017).
[24] C. Dong, X. Zheng, J. Li, D. Guo, L. Wu, X. Jiang, D. Xue, IEEE Transactions on Magnetics **49**(7), 4238 (2013).
[25] S. O. Aisida, P. A. Akpa, I. Ahmad, M. Maaza, F. I. Ezema, Physica B: Condensed Matter **571**, 130 (2019).